Electronic Supplementary Material (ESI) for Materials Horizons.

Supporting Information

Assessing the roles of mechanical cracks in Ni-rich layered cathodes on capacity decay of liquid and solid-state batteries

Xuedong Zhang[a], Zaifa Wang[b], Xiaomei Li[b], Yong Su[a], Zhangran Ye[b], Liqiang Zhang[b,*], Qiao Huang[a,*], Yongfu Tang[b,c,*], Jianyu Huang[a,b,*]

[a.] School of Materials Science and Engineering, Xiangtan University, Xiangtan, Hunan 411105, P. R. China

[b.] Clean Nano Energy Center, State Key Laboratory of Metastable Materials Science and Technology, Yanshan University, Qinhuangdao 066004, P. R. China

[c.] Hebei Key Laboratory of Applied Chemistry, College of Environmental and Chemical Engineering, Yanshan University, Qinhuangdao 066004, P.R. China.

Corresponding Author

*Correspondence to: jyhuang8@hotmail.com; tangyongfu@ysu.edu.cn;

qiaoh@xtu.edu.cn; lqzhang@ysu.edu.cn.

Supporting Figures

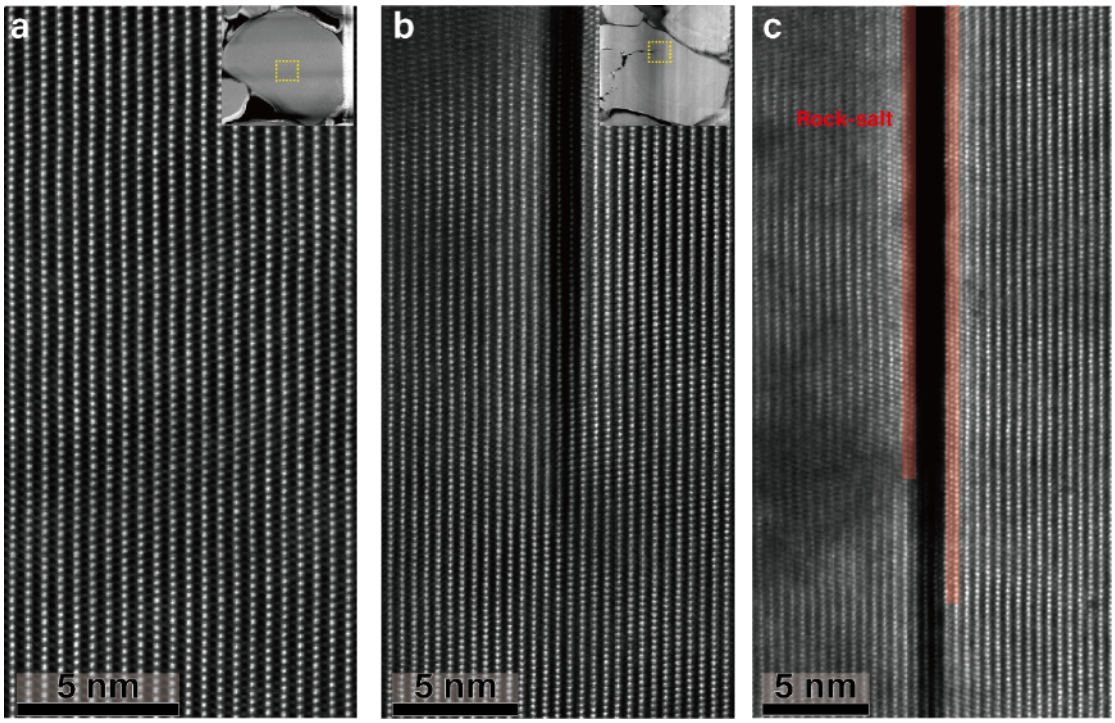

Figure S1. STEM-HAADF images of the pristine NMC811 before cycling (a) and after battery assembling at 700 MPa (b-c). Cracks were observed only after pressing. No rock-salt phase appears at the crack tip while 1-3 atomic layers of rock-salt phase exist on the surface of the crack.

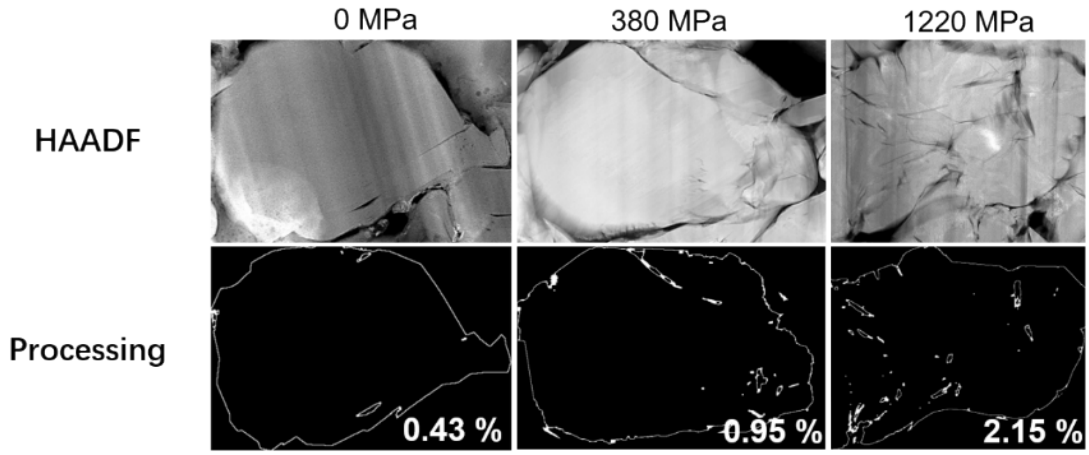

Figure S2. An image processing algorithm to extract the crack length and area. The area proportion of cracks in a single particle under various pressures was calculated. The proportions of crack area generated in the single particle of NMC811, NMC811-380 and NMC811-1220 is 0.43%, 0.95% and 2.15%, respectively.

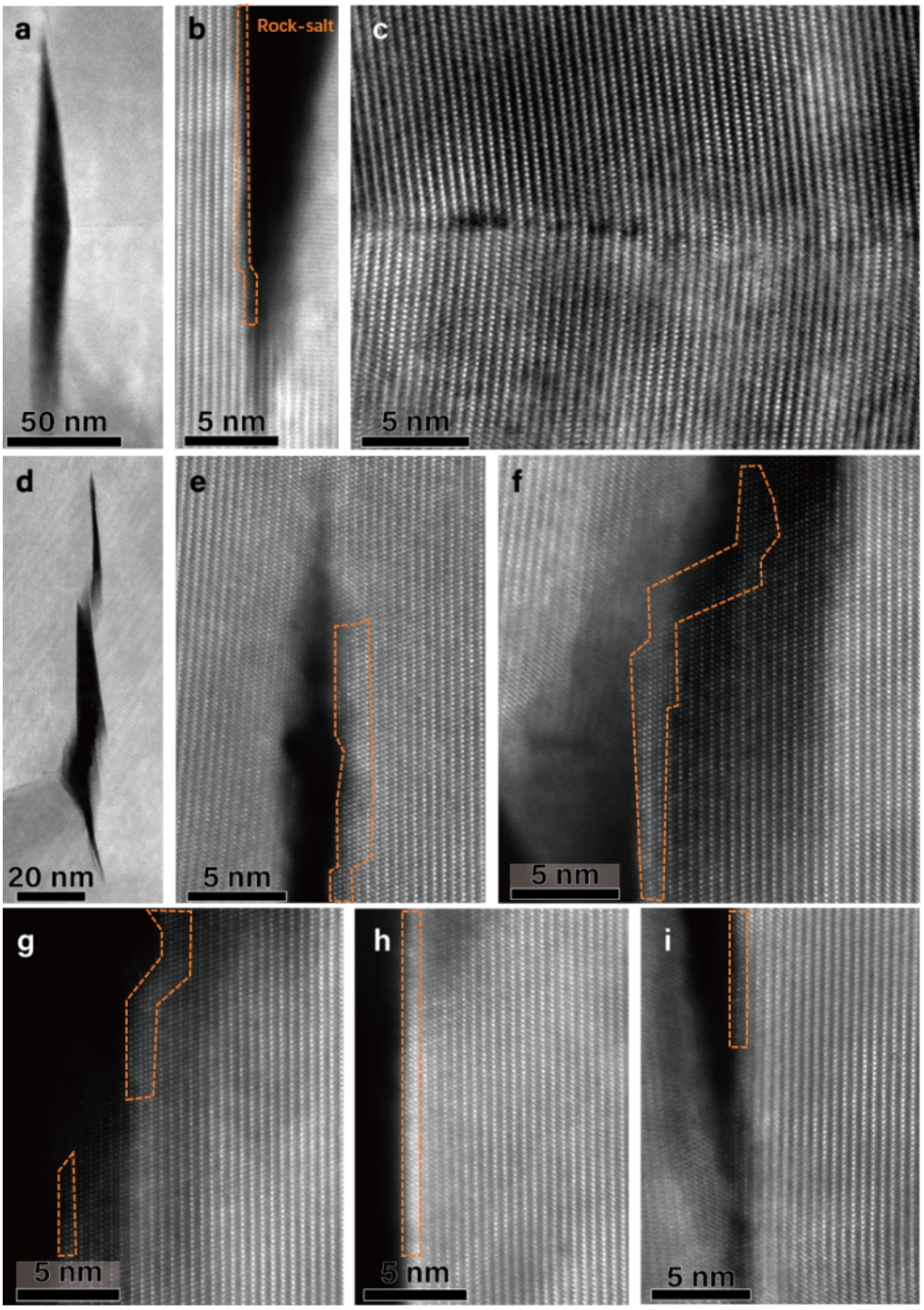

Figure S3. STEM-HAADF images of cracks parallel to the (003) plane in a NMC811-1220 sample before cycling. (a, d) Low magnification images of two mechanical cracks. (b-c, e-i) High magnification image of crack surfaces. Thin layers of rock-salt phase exist at the surfaces of the cracks. Note that small-angle grain boundaries were generated in (c) and (f). In (f) the upper and lower grains are connected by a thin stripe of rock-salt phase.

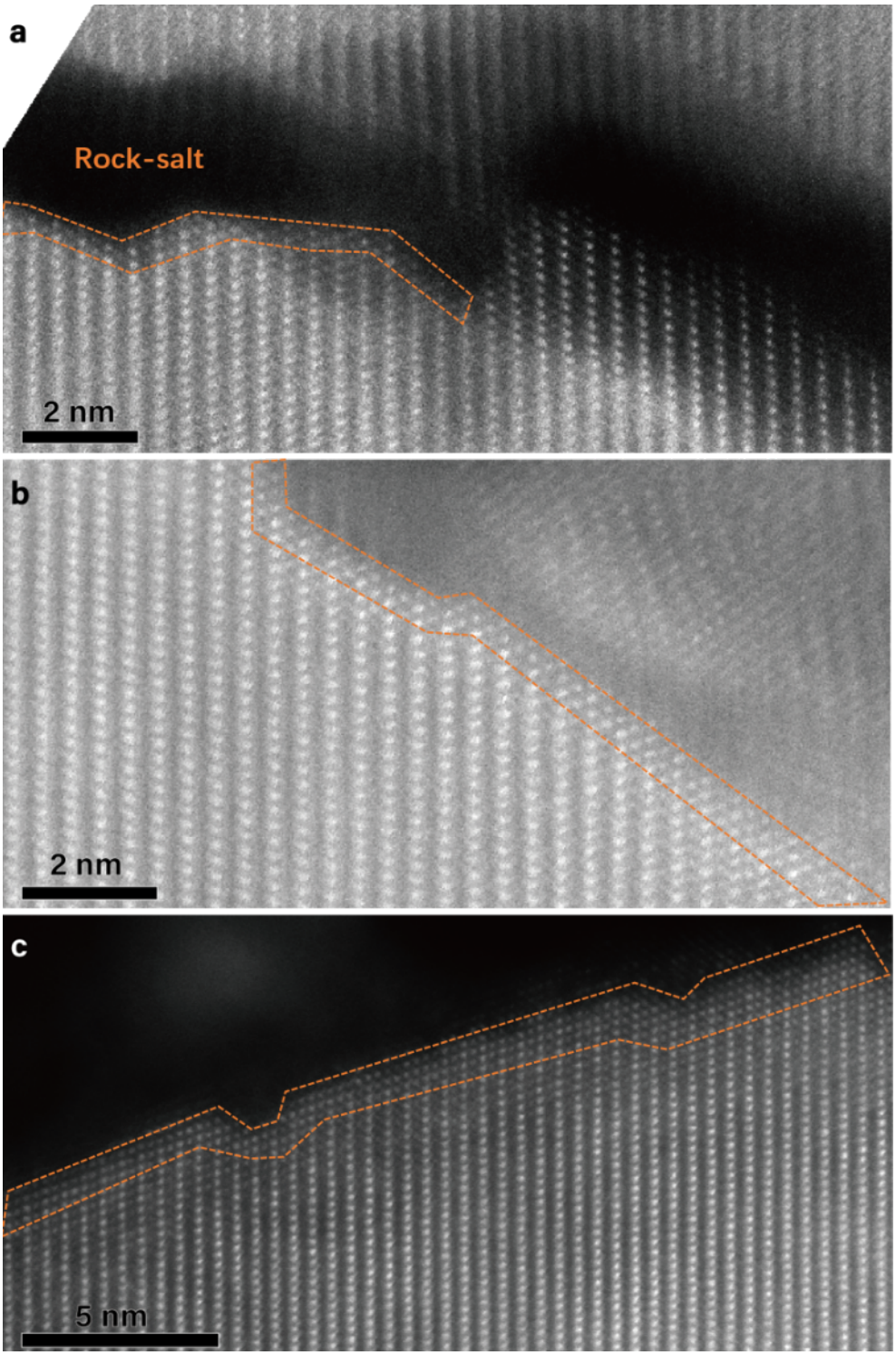

Figure S4. STEM-HAADF images of cracks along slanted (003) plane of NMC811-1220 before cycling. (a-c) Saw-teeth shaped fracture surfaces with thin layers of rock-salt phase are present. Note that large-angle grain boundary was generated in (b).

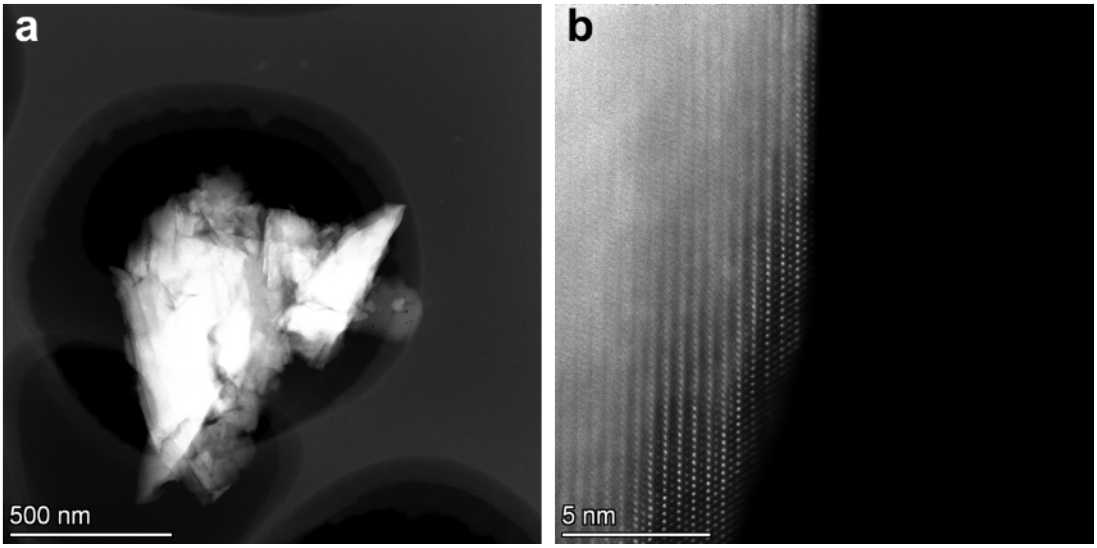

Figure S5. HAADF-STEM images of the NMC811-1220 sample prepared by crushing the NMC particles and spreading the broken particles directly onto the copper grid under argon gas protection. (a) Low magnification image of NMC particles. (b) Atomic-level HAADF-STEM image of the crack surface of the sample shown in Figure S5a. A thin layer of rock salt phase presented on the crack surface is similar to that of the FIB processed sample. In this study, two main potential sources for generation of rock salt phase were identified: 1) direct exposure of the NMC samples to air during sample transfer, and 2) sample damage caused by FIB preparation. To avoid the first source, all TEM samples were transferred through a vacuum transfer system, avoiding the influence of air. As for the second source, instead of FIB-preparation, we spread the crushed NMC powder directly on the TEM copper mesh to characterize the sample. We detected similar thin layer of rock salt phase on the freshly cracked surface of the NMC particles as found in the samples processed with the FIB preparation. Therefore, we believe that no additional rock salt phases were generated during the TEM sample transfer process, neither the sample was damaged during the FIB preparation.

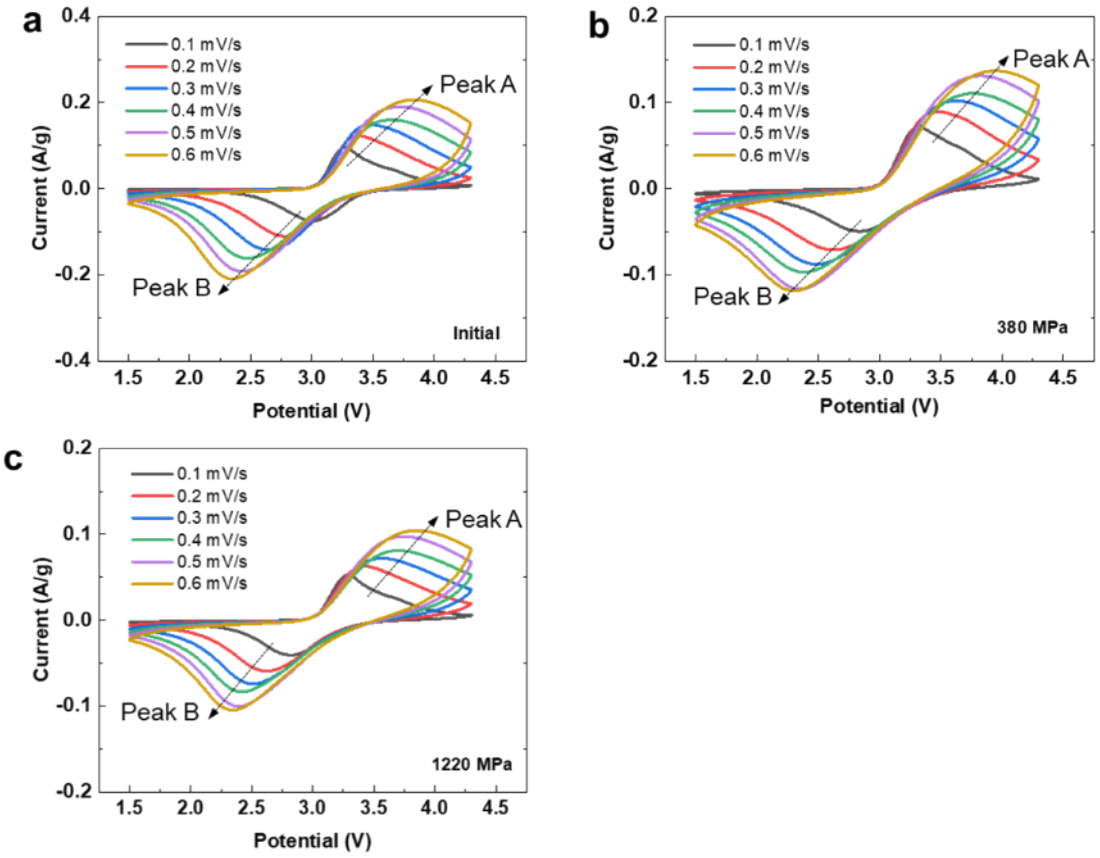

Figure S6 (a-c) CV curves of NMC811 (a), NMC811-380 (b), and NMC811-1220 (c) at different scan rates in ASSBs.

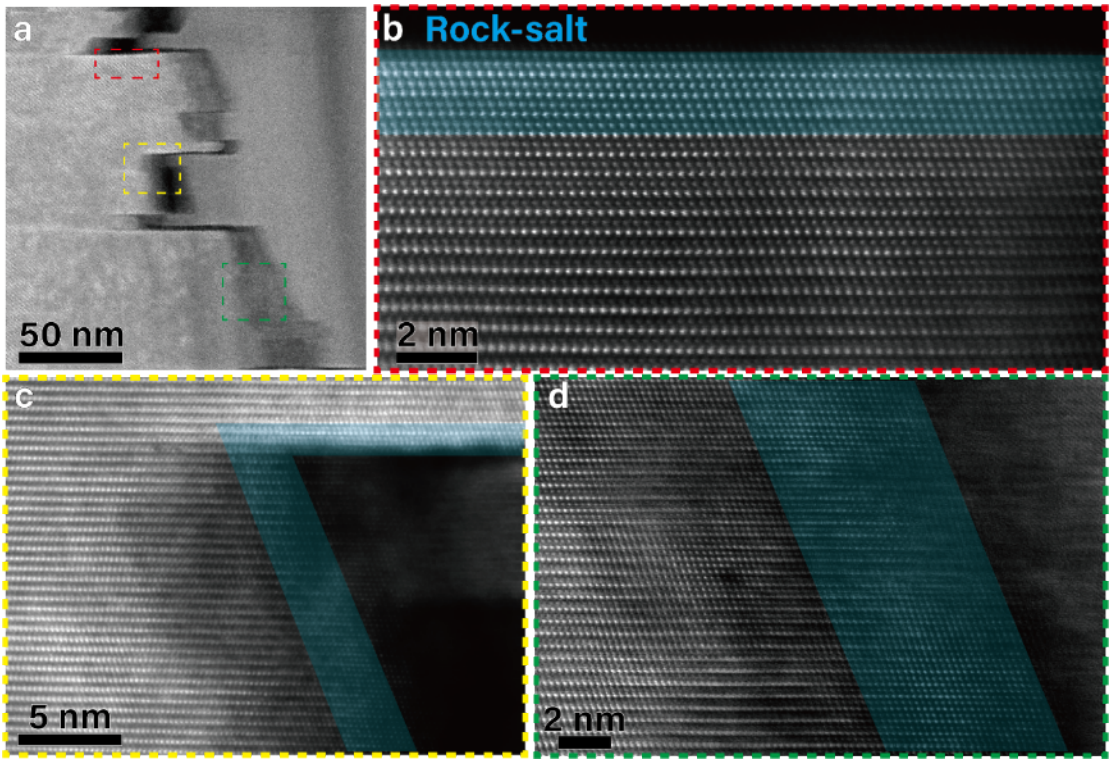

Figure S7. STEM-HAADF images of a mechanical crack along slanted (003) planes in the pristine NMC811 after 900 cycles in ASSBs. Low magnification photo of slanted crack (a); Thickness of rock salt phase in different directions (c); The rock-salt phase at the slanted planes (d) is slightly thicker than that at the surfaces of the (003) plane (b).

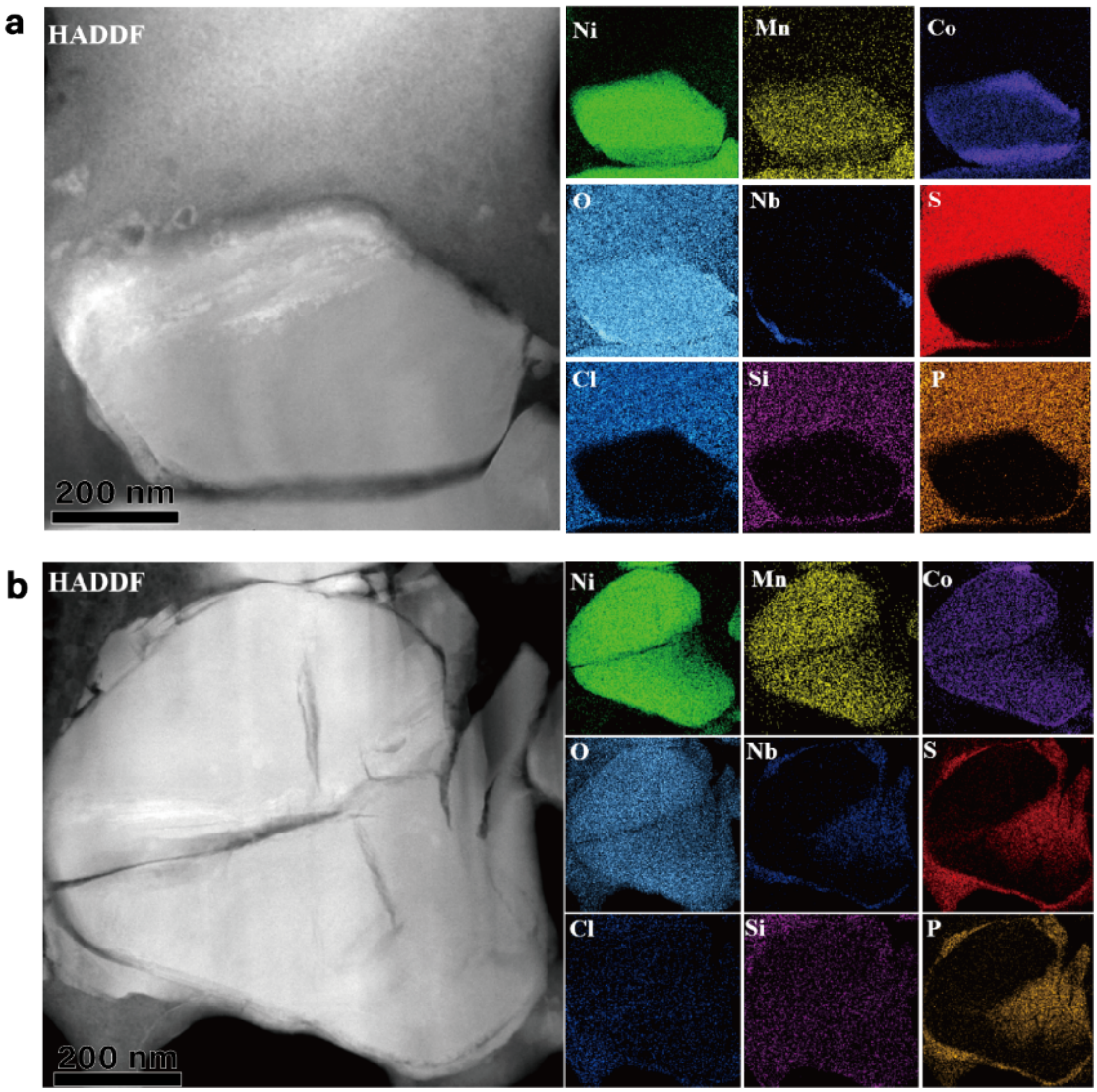

Figure S8. The EDS element mapping of single pristine NMC811 after 900 cycles in ASSBs. (a) Without cracks. (b) With cracks. No SSE was detected in the crack.

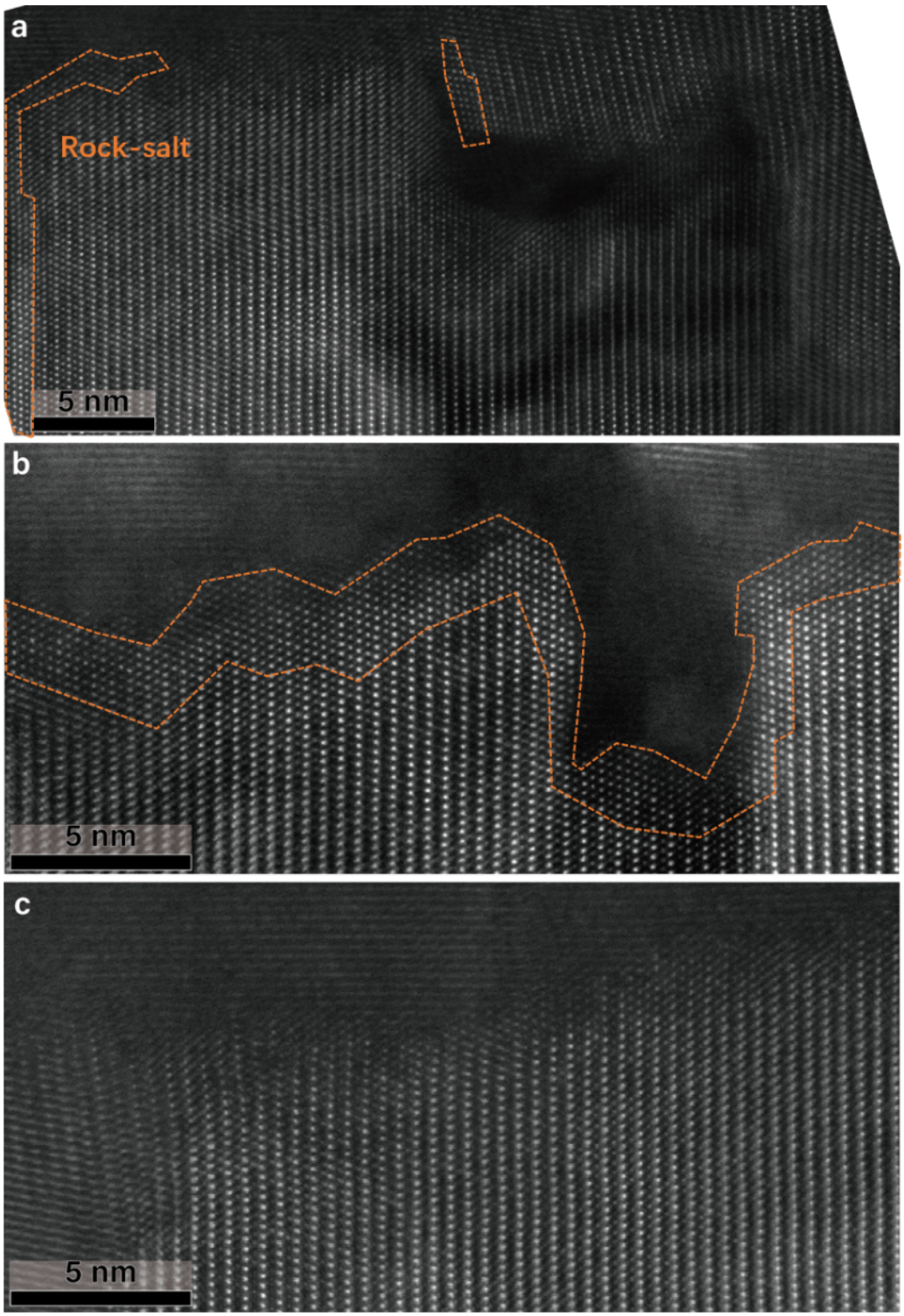

Figure S9. STEM-HAADF images of cracks surface slanted to (003) plane of NMC811-380 after 500 cycles in ASSBs. The thickness of the rock-salt phase remained about 1-2 nm. Note the upper grain is tilted with respect to the lower grain in (a).

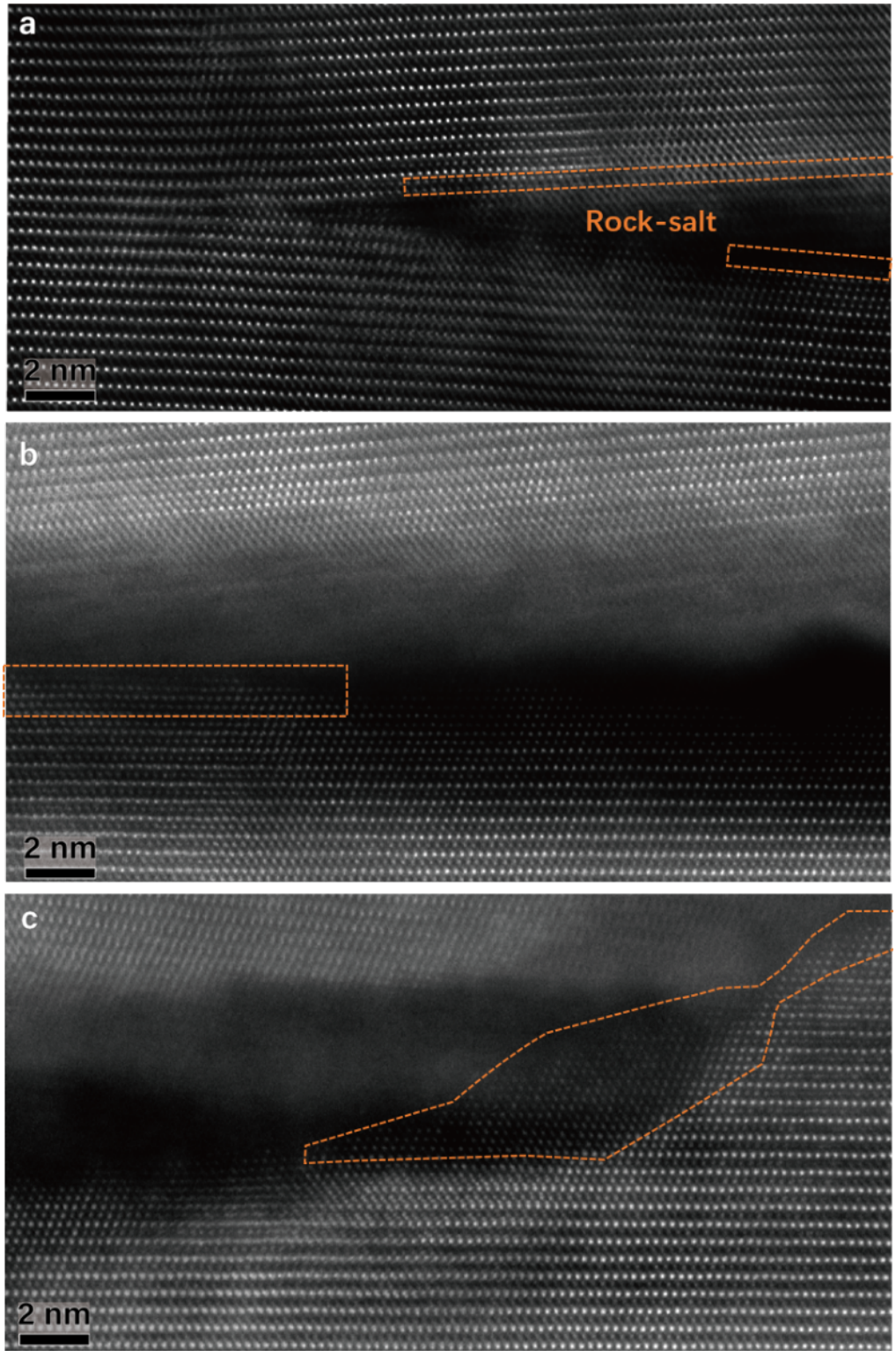

Figure S10. STEM-HAADF images of cracks surface parallel to the (003) plane in NMC-380 after 500 cycles in ASSBs. The thickness of the rock-salt phase remained about 1 nm. In (a) the crack tip is visible. No large deformation was observed at the crack tip. The (003) planes above and below the crack is tilted about 5°.

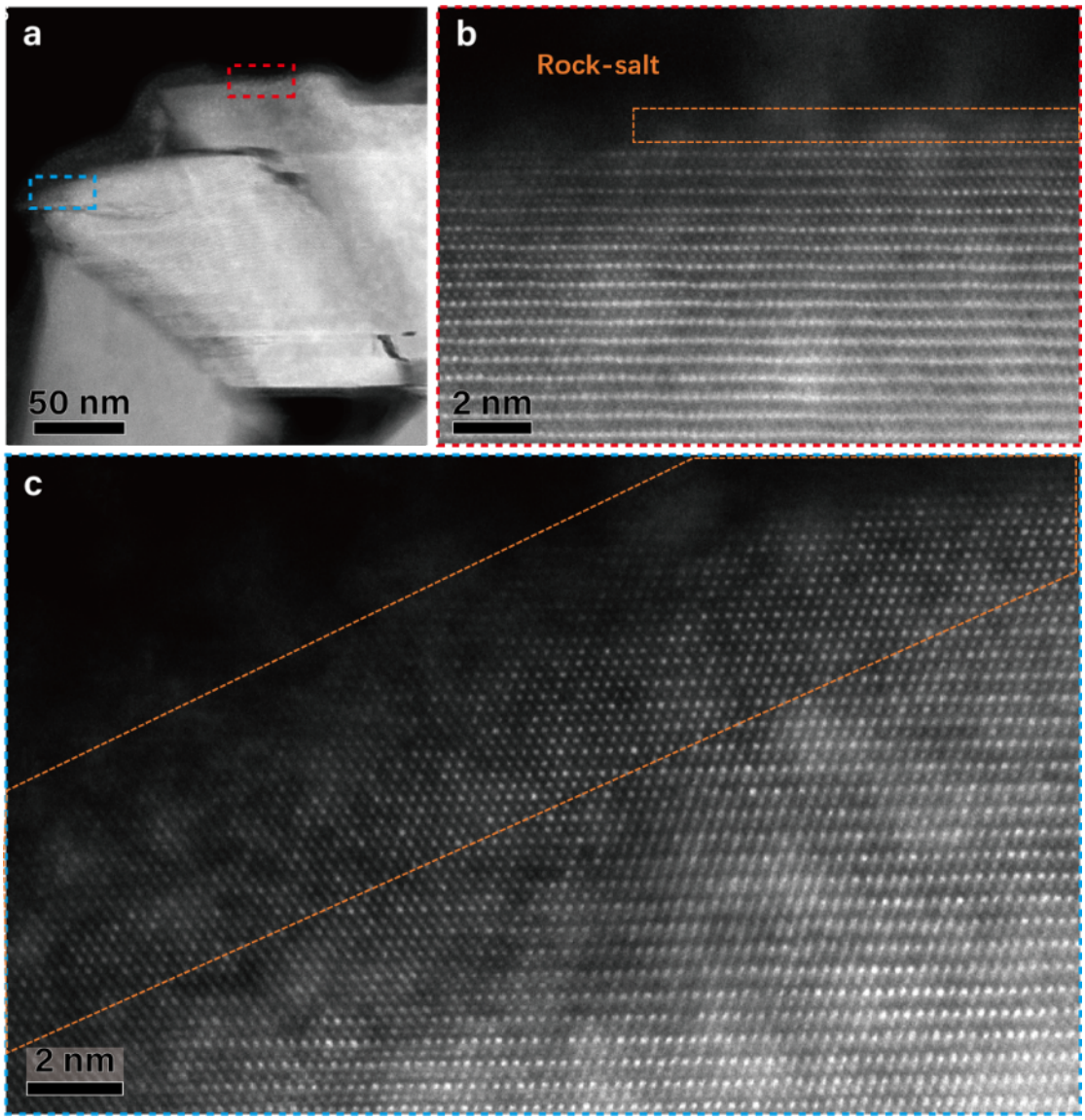

Figure S11. STEM-HAADF images of the particle surfaces parallel (b) and slanted (c) to (003) plane in NMC-380 after 500 cycles in ASSBs. The thickness of the rock-salt phase increased more along the slanted planes (2-5 nm) than that along the (003) planes (1 nm).

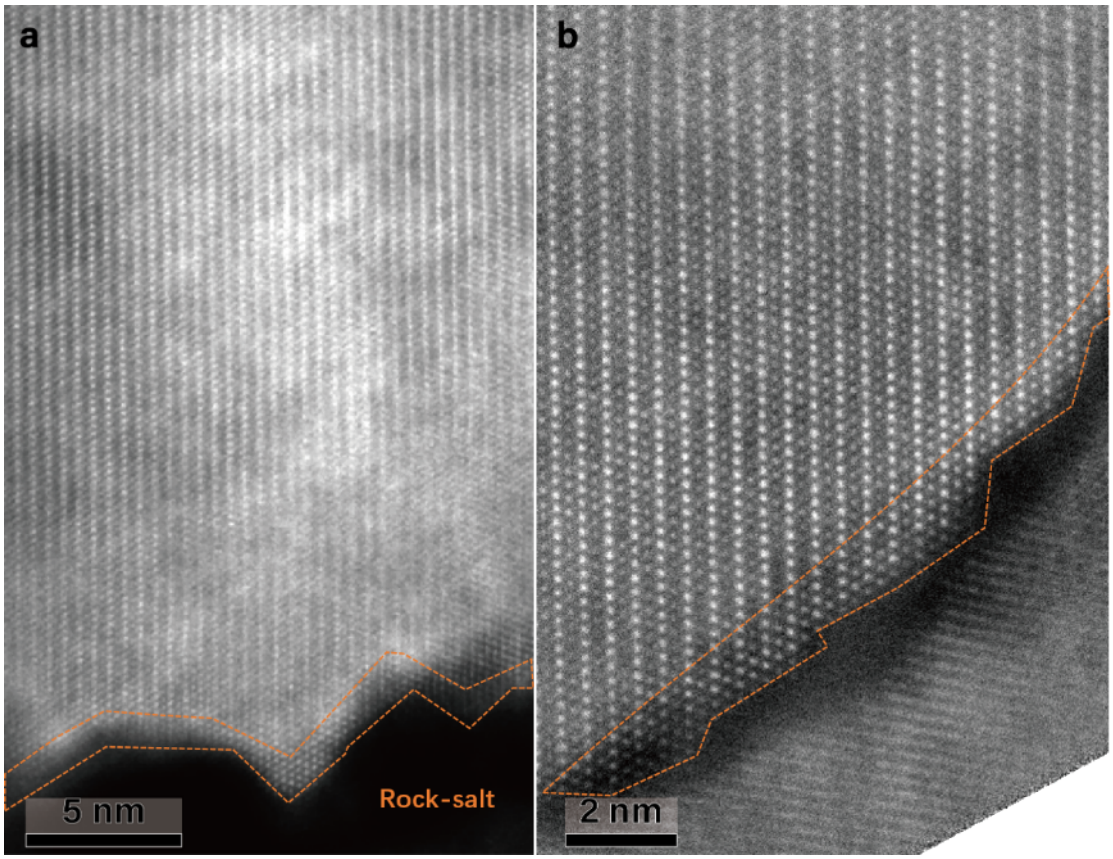

Figure S12. STEM-HAADF images of cracks surface slanted to (003) planes in NMC-1220 after 500 cycles in ASSBs. The thickness of the rock-salt phase remained about 1nm.

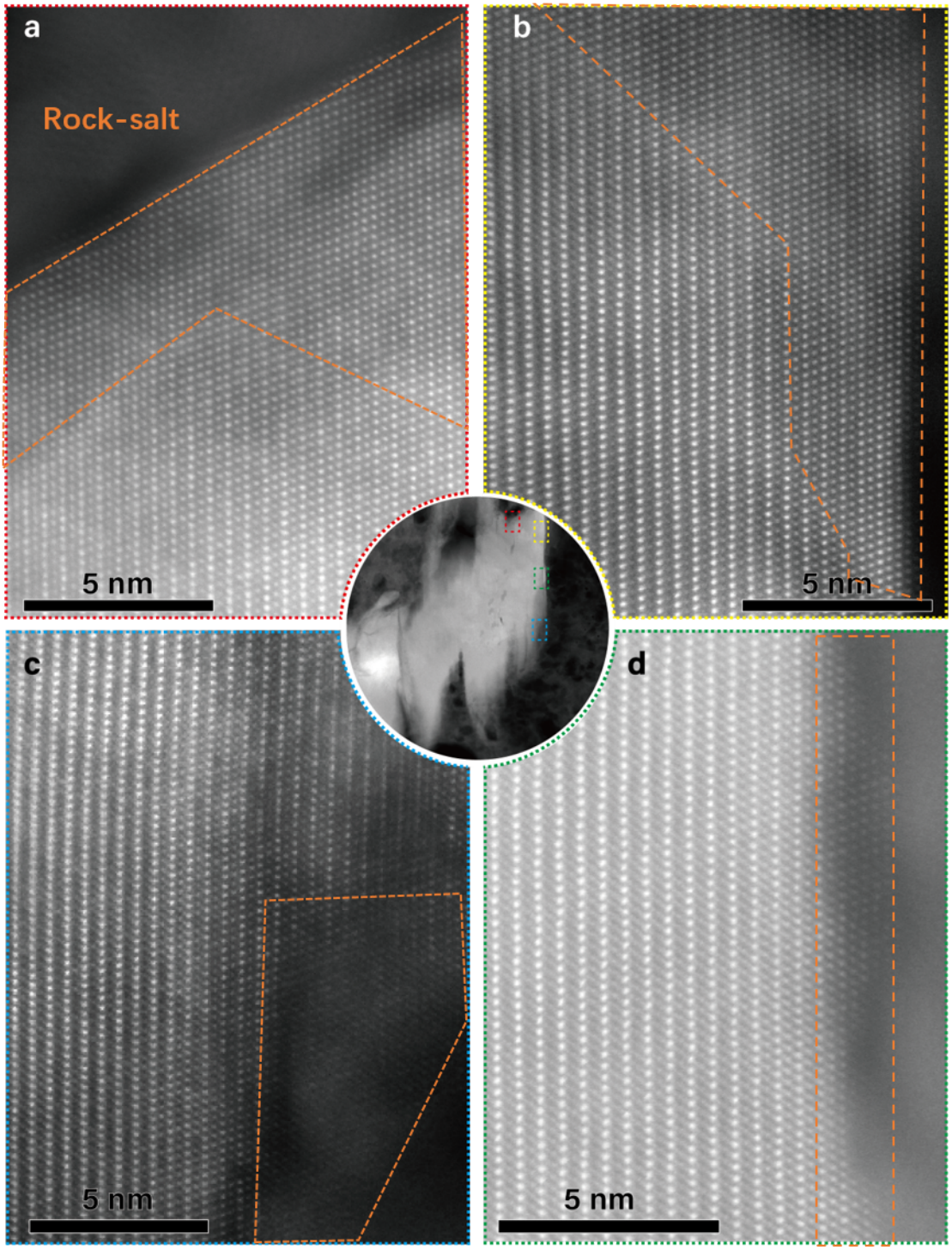

Figure S13. STEM-HAADF images of the particle surfaces slanted (a, c) and parallel (b, d) to the (003) planes in NMC-1220 after 820 cycles in ASSBs. The thickness of the rock-salt phase increased more along the slanted planes (4-10 nm) than that along the (003) planes (1-2 nm).

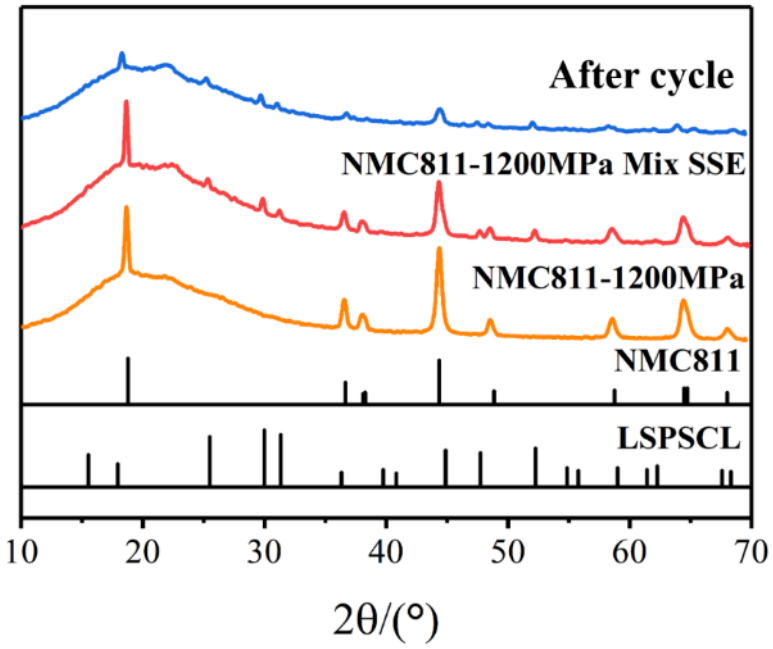

Figure S14. XRD characterization of the pristine NMC particles, NMC811-1220, and NMC-1220 mixing with the sulfide electrolyte before and after cycling. We conducted X-Ray Diffraction (XRD) analysis to characterize the cathode materials (NMC811 and NMC811-1220 MPa) before and after cycling (Fig. S14). The results indicate that there was no change in the peak position of NMC811-1220 when compared with the original NMC811, indicating that no phase change had occurred during the application of pressure. The results of the post-cycling analysis indicate a reduction in intensity and displacement of the (003) diffraction peak. This phenomenon can be attributed to either deformation or structural imperfections in the crystalline structure. Furthermore, the observed shift in the peak position may result from changes of atomic configurations or lattice constants. Upon conducting a HAADF-STEM characterization of the cycled samples, rock salt phase was discovered at the surface of the samples.

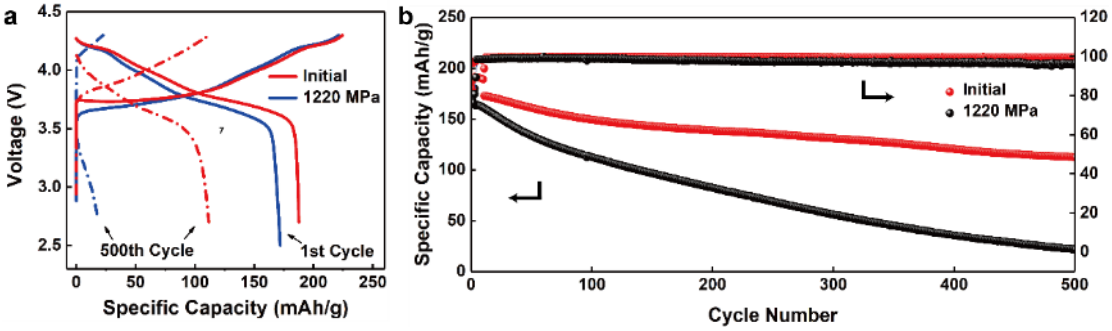

Figure S15. Electrochemical characterizations of the LELIBs. (a-b) Electrochemical characterization of the LELIBs: Charge and discharge profiles (a); Cycling performance of the LELIBs (b). Dramatic capacity decay was observed.

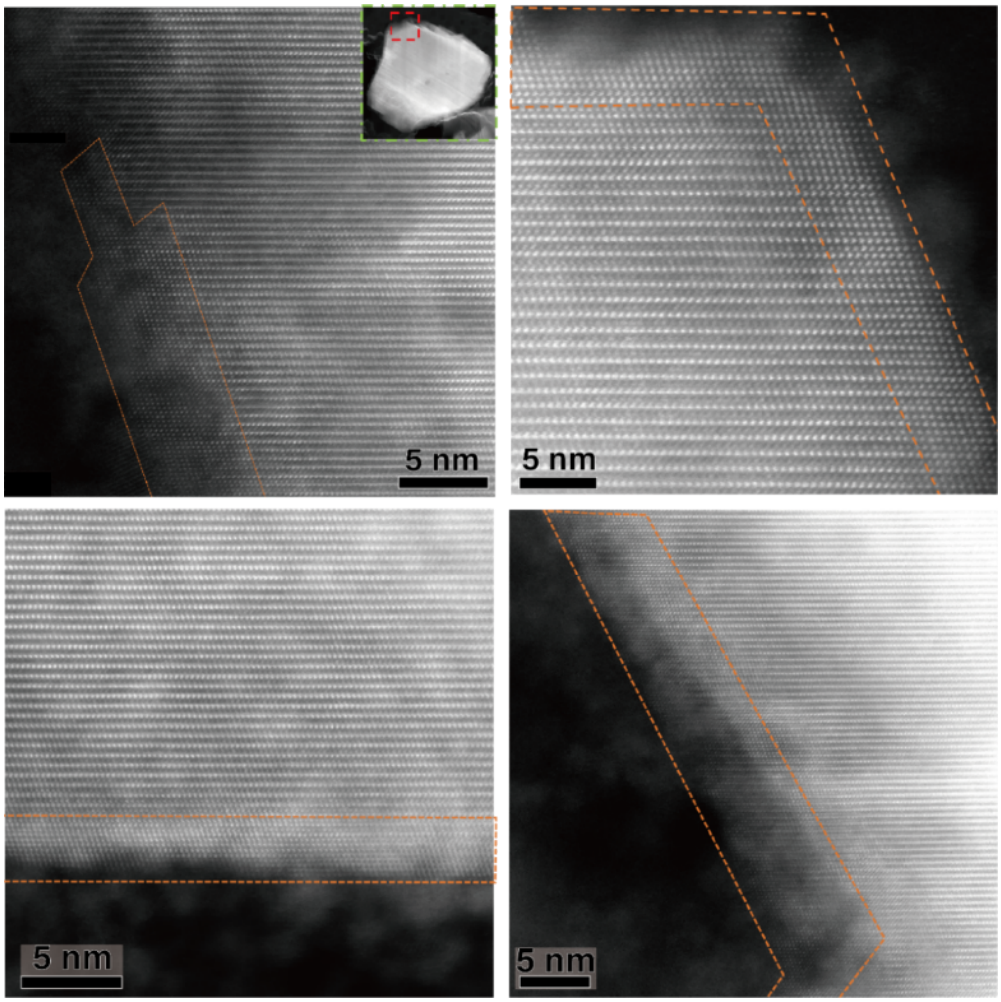

Figure S16. STEM-HAADF images of the particle surfaces slanted to (003) plane in NMC-1220 after 500 cycles in LELIBs. Rock-salt phase with a thickness of 2-6 nm was detected.

Supporting Table

Table S1 The thickness (nm) of the rock-salt phase in different samples after cycling.

		Crack surfaces	Particle surfaces	
			Parallel to (003) plane	Slanted to (003) plane
Solid state	Pristine	0.5~1	1~2	3~6
	380MPa	0.5~2	1~2	4~6
	1200MPa	0.5~1	1~2	4~10
Liquid state	Pristine	-	1~3	2~6
	1200MPa	2~4	1~3	2~6